Compact 2x2 and 4x4 MIMO Antenna Systems for 5G Automotive Applications

Mohamed O. Khalifa, Ahmad M. Yacoub, and Daniel N. Aloi

Department of Electrical Engineering
Oakland University, Rochester, Michigan 48309, USA
MKhalifa@Oakland.edu, Ahmadyacoub@Oakland.edu, Aloi@Oakland.edu

Abstract ─ In this paper, three Vehicular multiple-input multiple-output (MIMO) 5G antenna systems have been constructed from using a newly developed 5G cellular branched Monopole element are presented. The MIMO systems operates in the 5G frequency bands (617MHz-5GHz) with a compact structure that allows for up to four elements to be integrated in the same Sharkfin. The 3 configurations of MIMO systems have been simulated using HFSS, measured on a 1-meter ground plane (GND), then measured on a vehicle roof and the individual antenna parameters in terms of reflection coefficient and efficiency have captured. The MIMO antenna systems performance in terms of passive isolation, combined radiation pattern, envelope correlation coefficient (ECC), and diversity gain (DG) have been reported and discussed.

Index Terms ─ Automotive antennas, correlation coefficient, 5G, 2x2 and 4x4 MIMO systems.

I. INTRODUCTION

With the expansion of the cellular systems being integrated in cars to support the connected vehicle effort, a need for multiple antennas support wireless service has emerged. The Multiple Input Multiple Output (MIMO) system consists of two antennas or more that receive or transmit multiple layers of orthogonal data streams from cellular base stations which allow for increased channel capacity, data rate and the total throughput of the system without increasing the operating frequency band or the transmit power [1]. To this date, 2X2 MIMO configuration with de-correlated antennas that receive two data streams is being used to realize downlink reception in modern vehicles [2]. The performance of the MIMO system is highly dependable on the efficient design of the MIMO antennas that should low correlation between them and a high total antenna efficiency [3].

An important characteristic of the communication systems is the ECC between received signals of the antennas that construct the MIMO system. Small ECC values are crucial to increase transmission capacity as well as to improve the multipath fading. ECC tells how

independent MIMO antennas radiation patterns are, for example, for a 2X2 MIMO system, if one antenna is vertically polarized and the other one is horizontally polarized then the ECC value will be 0. There are 2 ways to calculate the ECC in a MIMO system [4], the first method used S parameters to find ECC and it assumes lossless/60% or more efficient antennas which is unrealistic. Whereas the second method (which is more accurate) used throughout this paper utilizes radiation patterns of individual antennas to calculate the ECC of MIMO system. Modern vehicles are equipped with multiple wireless services such as Global Navigation Satellite Systems (GNSS), Remote Keyless Entry (RKE), Satellite Digital Audio radio service (SDARS), etc. [5]-[7]. Each of these services requires dedicated antennas and it is unfeasible to distribute them all over the vehicle and consequently they all integrated in a single package (Sharkfin). Since the available space with the Sharkfin for each antenna is much smaller than the wavelengths at the which the antenna expected to operate, issues such as antenna size and bandwidth limitations as well as passive port isolation between different elements within the Sharkfin will take place. Furthermore, the Sharkfin size limitation will also impact the port isolation and correlation of MIMO antennas and impose some challenges to design an antenna system that satisfies the diversity requirements [8],[9].

In [10], [11], 2X2 MIMO systems based on Monopole and PIFA elements respectively have been introduced, however the bandwidth of operation is very small (700-925MHz). The 2X2 MIMO systems bandwidth have been increased to cover from 790MHz to 3GHz with reasonable antenna dimensions and an ECC of less than 0.3 and 0.05 in [12] and [13] respectively but the bandwidth of operation doesn't cover 5G frequencies (617MHz-5GHz). In [14]-[18], the authors have developed 2X2 MIMO structures that are constructed from either Monopoles or PIFA elements with a less than 0.5 ECC however, these MIMO systems are only covering LTE (698MHz-3GHz) frequency bands and not 5G frequencies. A much broader

bandwidth (700MHz-6GHz) with less than 0.16 of ECC (using first method in [4]) is achieved by authors in [19] but it doesn't include the B71 band (617MHz-698MHz) as well as it comes at an increased volume $(70 \times 70 \times 29 mm^3)$ which makes it impossible to fit in production Sharkfins. Finally, a 4X4 MIMO system is presented in [20], However, B71 frequency band is not included (which will introduce a big challenge trying to fit the antenna in a sharkfin), there are no information about system volume, and also the work has not been supported by either ground plane or vehicle measurements data. Several studies outside the automotive industry have targeted decoupling antennas in a MIMO system packaged in a small volume with various techniques like the use of electromagnetic band gap (EBG) structures [21], Ceramic Superstrate-Based Decoupling Method [22], and metamaterials [23]-[27]. The automotive MIMO systems presented in this work do not require a special decoupling mechanism. In fact, decoupling of antennas is obtained by mainly using spatial and pattern diversity at the low and high band respectively which puts more burden on compactness and performance of building block antenna element.

This work introduces three novel MIMO structures; configuration I of a 2x2 MIMO antenna system, configuration II of a 2x2 MIMO antenna system, and a 4x4 MIMO antenna system. The three structures are mainly developed for automotive industry to cover 5G cellular frequencies (617MHz-5GHz), fit in a car roof sharkfin, and have an inherited GNSS frequencies rejection which makes it easy to integrate with other antennas within a sharkfin. In this work, HFSS has been used to simulate the 3 MIMO systems configurations, then the systems have been measured inside and anechoic chamber on ground plane and on a vehicle roof. The antennas important parameters such as of reflection coefficient, isolation, total efficiency, radiation pattern have been captured. Then an Octave code is used to calculate the ECC and DG from the captured data.

The work in this paper is organized in two sections: Section II explains the theory about correlation coefficient and diversity gain calculation equations and it also shows the design goals. Section III presents the proposed 2x2 MIMO configurations, the novel 4x4 MIMO system, and finally a comparison between proposed systems and available work in literature.

II. MIMO ANTENNA SYSTEMS PERFORMANCE METRICS

All the most important metrics in MIMO antenna systems are ECC and DG. The ECC can be related to the electric field radiation pattern through the equation in [4] as below:

$$\rho_{e,ij} = \left| \frac{\int_0^{2\pi} \int_0^{\pi} (XPR \cdot E_{\theta i} \cdot E_{\theta j}^* \cdot P_\theta + XPR \cdot E_{\phi i} \cdot E_{\phi j}^* \cdot P_\phi) \sin(\theta) \, d\theta d\phi}{\sqrt{\prod_{k=i,j} \int_0^{2\pi} \int_0^{\pi} (XPR \cdot E_{\theta k} \cdot E_{\theta k}^* \cdot P_\theta + XPR \cdot E_{\varphi k} \cdot E_{\varphi k}^* \cdot P_\phi) \sin(\theta) d\theta d\phi}} \right|^2, (1)$$

where $E_{\theta i}$ and $E_{\theta j}$ are the values of electric field in the theta axis while $E_{\phi i}$ and $E_{\phi j}$ are the values of electric field in phi axis. XPR is the cross-polarization discrimination factor tells the difference between incident electromagnetic wave vertical and horizontal polarization. P_θ and P_ϕ are the theta and phi power densities. Equation (1) can be simplified by setting XPR = 1 assuming uniform power densities.

The other MIMO system performance metric is the DG which is defined as the quantified improvement in signal-to-noise ratio (SNR) by the receiving signals from the MIMO antennas and usually calculated in dB. The DG can be calculated as in [28]:

$$DG = DG_0 . DF . K, \qquad (2)$$

where DG_0 is the ideal case diversity gain which is 10dB. DF is the degradation factor which shows how much the ECC impacts DG and is calculated as: $\sqrt{(1-\rho)}$. K represents the ratio of the mean effective gain (MEG) between the MIMO antenna elements ($K = MEG_i/MEG_j$). MEG is the effective gain ratio at the antenna element, in other words MEG is the received to incident power ratio at the element. (K~=1) condition should be satisfied for received signals by MIMO systems assuming good channel characteristics.

III. COMPARATIVE STUDY OF THE PROPOSED MIMO SYSTEMS

In this section, three different MIMO antennas configurations are being studied. The building block for each configuration is the branched Monopole element in Fig. 1. The MIMO configurations are then simulated and measured on a 1-meter ground plane and on a vehicle's roof inside an anechoic chamber. The obtained data from simulations and chamber measurements are directly reported whereas ECC and DG results are generated using Octave software for each MIMO configuration in this section. Table 1 shows general design guidelines:

Table 1: Design guidelines

Parameter	Value
Polarization	Vertical Linear Polarization (VLP)
Reflection Coefficient	-5.4dB (3.3VSWR) at 5G bands
Avg. Total Efficiency	60%
Isolation	Minimum 10dB across 5G bands
ECC	Less than 0.5

A. Configuration I of a 2x2 monopole-based MIMO system

Figure 1 shows the Monopole element that will be used construct high order MIMO structures. The antenna functions in the 5G frequency bands (617MHz-5GHz).

Multiple current paths have been realized by adding 2 arms to the antenna covering 5G frequencies of interest. Band (617 MHz – 960 MHz) is mainly covered by Arm 1 currents whereas band (1.71-5 GHz) frequencies are radiated by Arm 2 as in Fig. 1. To obtain omnidirectional radiation pattern, high efficiencies, and good matching performance, Arm1 and Arm2 of the antenna are loaded at $\frac{\lambda_{LB}}{4}$ and $\frac{\lambda_{HB}}{4}$ distances from ground plane respectively where λ_{LB} and λ_{HB} are the mid-low and mid-high bands wavelengths respectively. The geometrical values of the building block antenna are shown in Table 2.
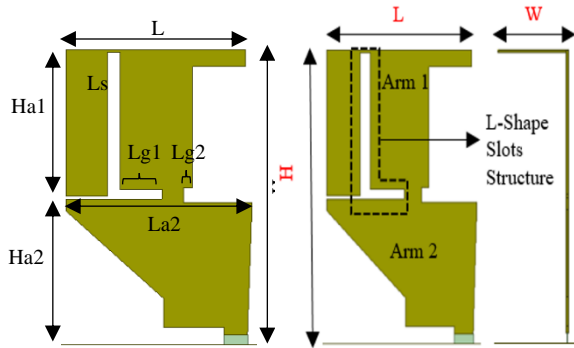
Fig. 1. Building block antenna with side and front views, arms structure, and antenna dimensions.

Table 2: Values of the geometrical parameters of MIMO systems building block antenna

Parameter	Value (mm)	Parameter	Value (mm)
H	60	Lg1	9
L	38.5	Lg2	2
W	14.9	Ls	2.6
Ha1	30	La2	39.8
Ha2	29.3		
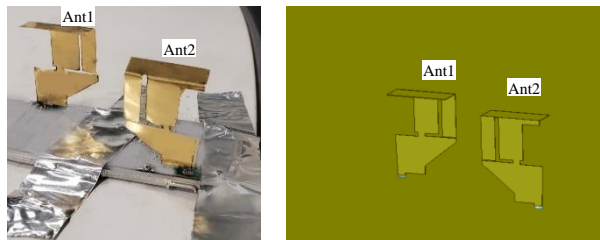
Fig. 2. Configuration I of a 2x2 MIMO system placement on vehicle roof and simulation setup.

The two Monopole elements were cut from a metal sheet and placed in such a way that will result in an omnidirectional combined radiation pattern as well as a minimal ECC value. The system is simulated then measured on 1-meter GND and on a car's roof with a port-to-port distance of 135mm (which is higher than $\frac{\lambda_{Lowest\_freq}}{2*\sqrt{\varepsilon_r}} = 114$mm on FR4 PCB with $\varepsilon_r = 4.4$) between Monopole elements. Figure 2 shows Configuration I of a 2x2 MIMO systems on a car roof.

The performance of Antenna1 (Ant1) and Antenna2 (Ant2) of this MIMO system has been reported in terms of reflection coefficient and isolation as in Fig. 3. Both antennas show an agreement between simulation and GND measurement. Good reflection coefficient values have been observed of a worse of -5.6dB and -6.4dB at 617MHz of Ant1 and Ant2 respectively with reasonable GNSS bands (1560MHz-1190MHz) rejection. Figure 3 also shows a good isolation between Ant1 and Ant2 in this configuration of a worse case 12dB (expressed as -12 dB in S21 format).

Next, the total efficiencies of Ant1 and Ant2 have been captured after a successful placement of the MIMO system on 1-meter GND and then on a car roof and the results are shown in Fig. 4. Both antennas exhibit higher efficiencies when placed on GND compared to placement on a car roof. It can be noticed that both antennas measured on GND have an average total efficiency of 79.8% across all 5G frequency bands while the average total efficiencies decrease to 74% and 71% when measured on a car roof for Ant1 and Ant2 respectively.

Simulation, GND measurement, and vehicle measurement of a combined MIMO system radiation pattern sample have been presented in Fig. 5. The sample represents a Gain theta horizontal cut at 80 degrees of theta and four frequencies namely 617MHz, 1900MHz, 3900MHz, and 5000MHz to provide a good idea about the system performance. The combined MIMO system pattern is obtained by measuring each antenna when the other antenna is loaded by a 50Ohm terminator and then combine the resultant individual antenna patterns selecting the maximum values of Gain theta between Ant1 and Ant2 measurements for a specific phi-frequency pair at 80 degree of theta. Finally, the average gain of the MIMO system combined radiation patterns measured on car roof is found to be -1.14dBi, 3.15dBi, 1.81dBi, and 2.84dBi at frequencies 617MHz, 1900MHz, 3900MHz, and 5000MHz, respectively.
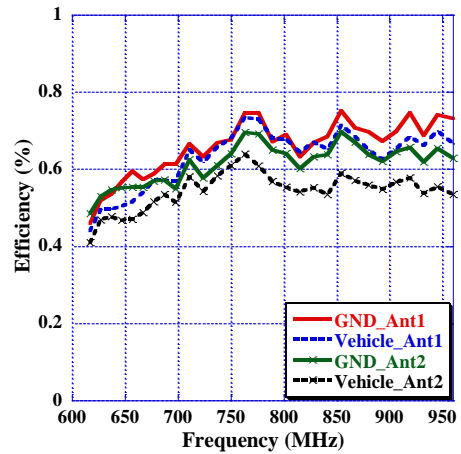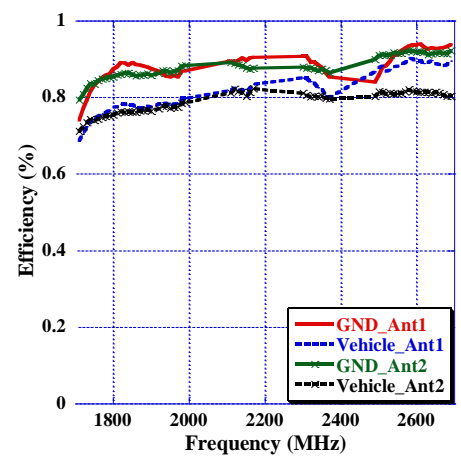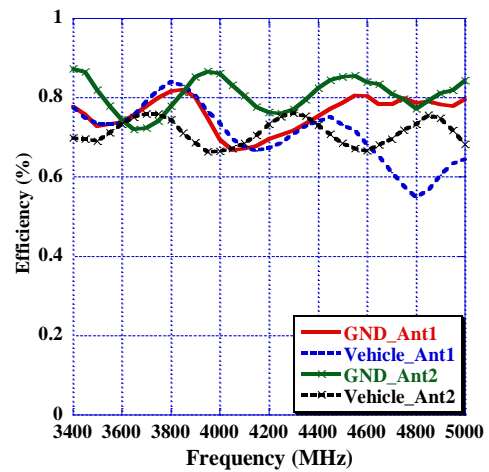
(a)

(b)

(c)
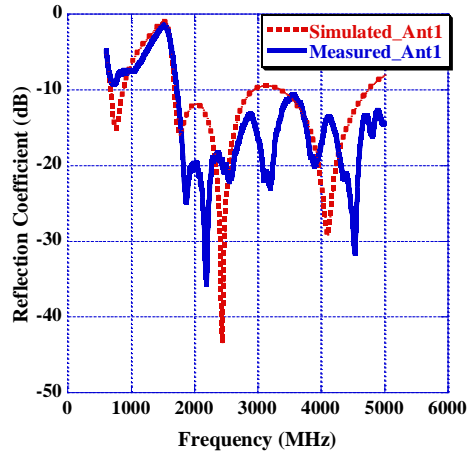
(a)
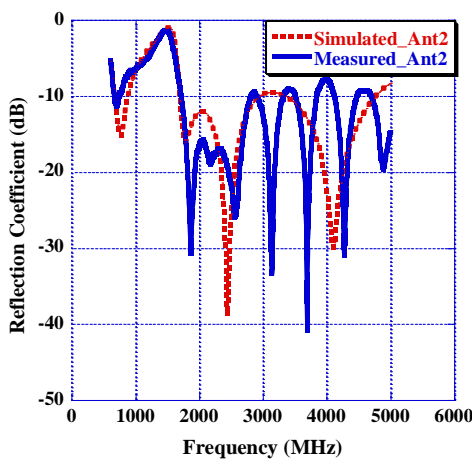
(b)
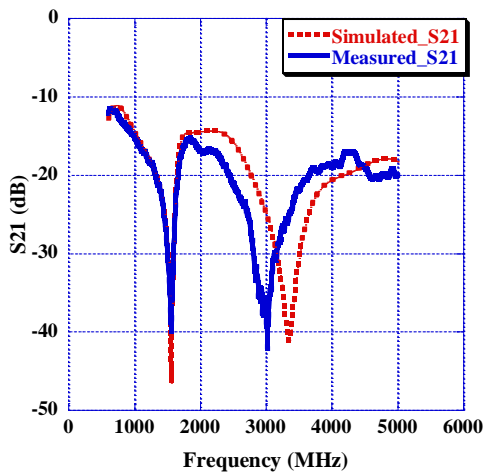
(c)

Fig. 3. Configuration I of a 2x2 MIMO system simulated and measured: (a) Antenna1 S11 in dB, (b) Antenna2 S11 in dB, and (c) S21 between Antenna1 and Antenna2 in dB.

Fig. 4. Antenna efficiency for Configuration I MIMO systems Monopoles measured on GND and on vehicle roof for frequency ranges: (a) 617-960MHz, (b) 1710-2690MHz, and (c) 3400-5000MHz.
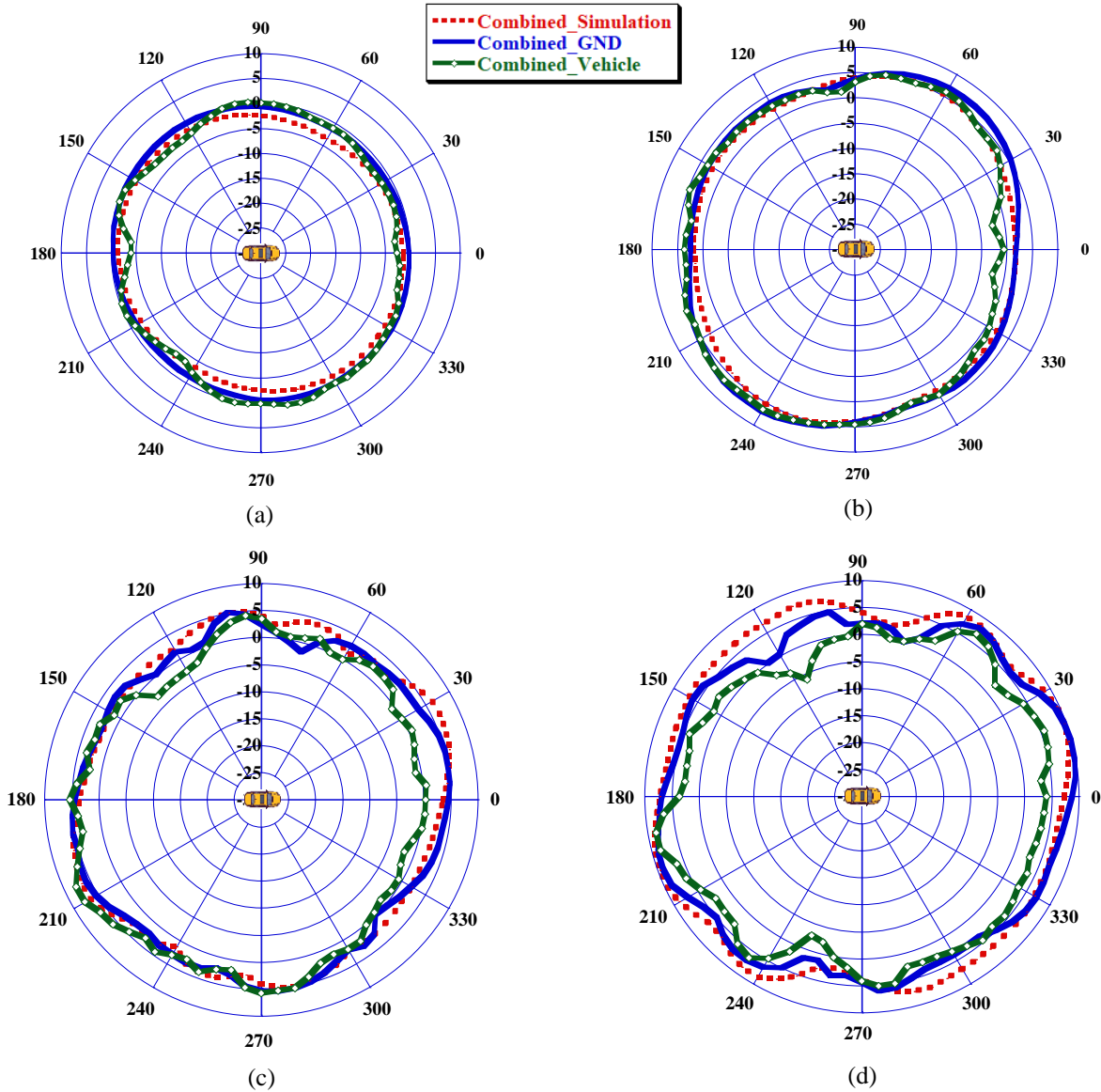
Fig. 5. Combined radiation pattern of simulation, GND measurement, and vehicle measurement in (dBi) at theta = 80 deg. for frequencies: (a) 617 MHz, (b) 1900 MHz, (c) 3900 MHz, and (d) 5000 MHz.

ECC and DG on GND and on car roof for configuration I of a 2x2 MIMO systems are depicted in Fig. 6 (a) and Fig. 6 (b) respectively. The two figures suggests that higher values of ECC and consequently lower values of DG occurs at low frequencies (i.e., 617MHz) because the wavelength is big which leads to more correlation between the antennas. In this MIMO configuration an ECC of better than 0.13 and a DG of better than 9.92dB have been realized.

(b)
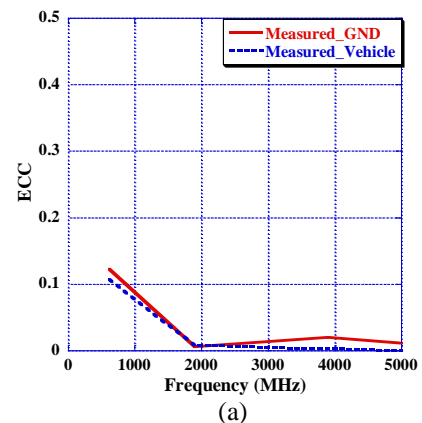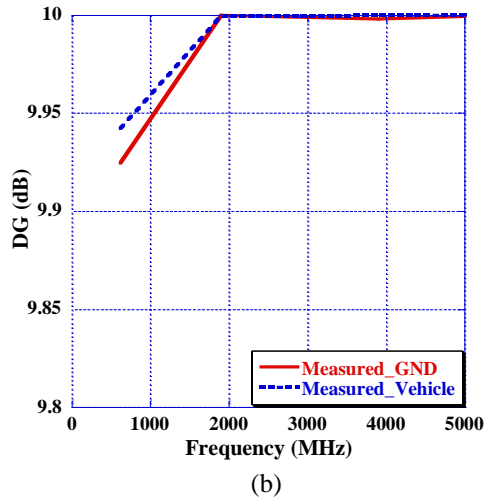
Fig. 6. Configuration I of a 2x2 MIMO system: (a) envelope correlation coefficient, and (b) diversity gain.

B. Configuration II of a 2x2 monopole-based MIMO system

Similar to Configuration I in subsection A, two Monopole elements have been placed on a Printed Circuit Board (PCB) with a distance of 125mm (from port to port) between them. The monopoles are place on the back of the roof of a car as in Fig. 7 to allow for an omnidirectional combined radiation pattern.

The performance of Ant1 and Ant2 of this MIMO system has been reported in terms of reflection coefficient and isolation as in Fig. 8. Both antennas show an agreement between simulation and GND measurement. Good reflection coefficient values have been observed from GND measurements of a worse of -7.4dB and -6.4dB at 617MHz of Ant1 and Ant2 respectively with reasonable GNSS bands rejection. Figure 8 also shows a good isolation between Ant1 and Ant2 in this configuration of a worse case 15dB (expressed as -15 dB in S21 format).
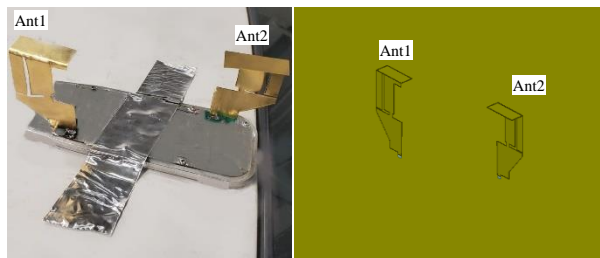

Fig. 7. Configuration II of a 2x2 MIMO system placement on vehicle roof and simulation setup.

A comparison of on GND and on vehicle measurements of Ant1 and Ant2 total antenna efficiencies in this configuration is illustrated in Fig. 9.
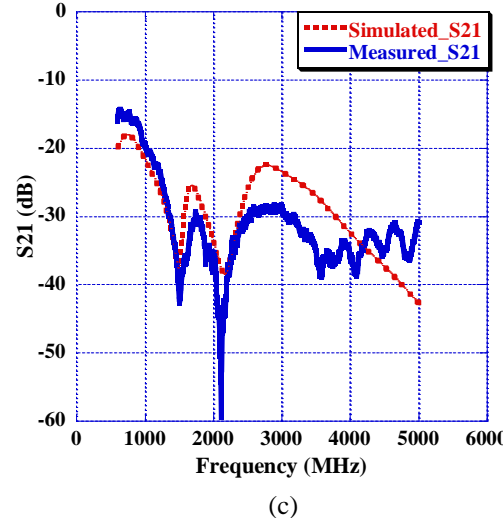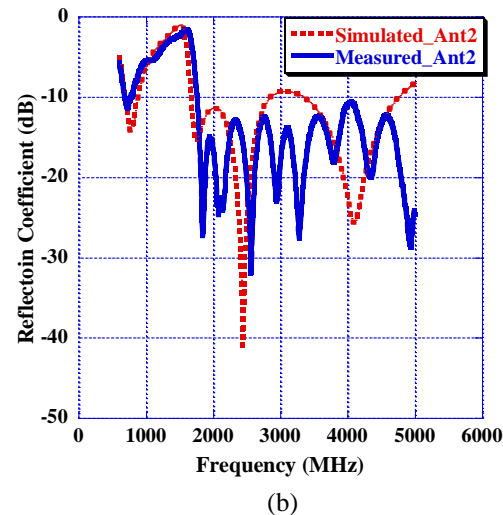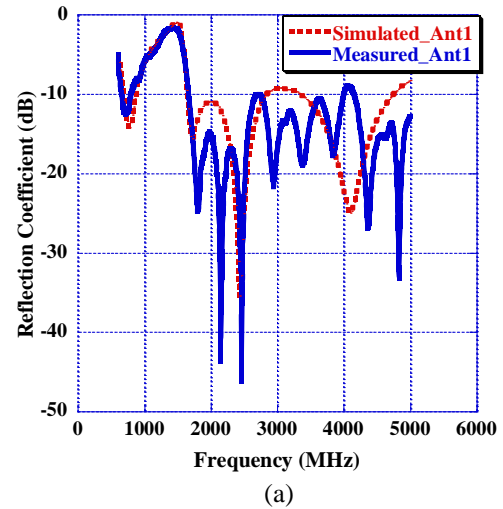

(a)

(b)

(c)

Fig. 8. Configuration II of a 2x2 MIMO system simulated and measured reflection coefficient for: (a) Antenna1, (b) Antenna2 in dB, and (c) S21 between Antenna1 and Antenna2 in dB.
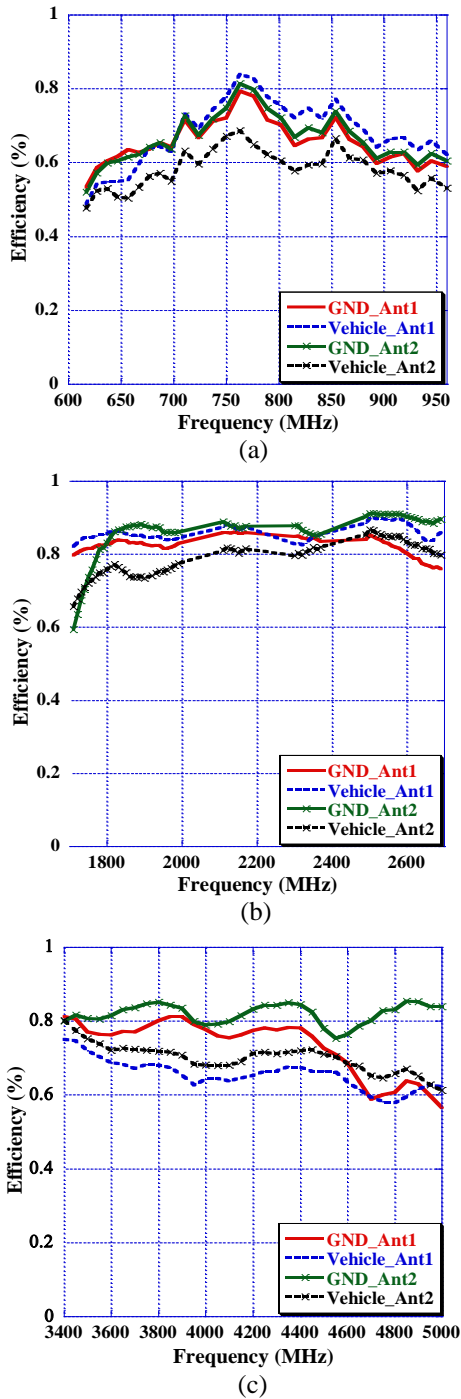
(a)

(b)

(c)

Fig. 9. Total antenna efficiency for Configuration II MIMO systems monopoles measured on GND and on vehicle roof for frequency ranges: (a) 617-960MHz, (b) 1710-2690MHz, and (c) 3400-5000MHz.

The GND measurement has an average efficiency higher than 76% for both elements across all 5G bands

whereas the vehicle measurement is 5% less namely an average total efficiency of 71.7%.

ECC and DG on GND and on car roof for configuration II of a 2x2 MIMO systems is depicted in Fig. 10 where an ECC of better than 0.02 and an approximately 10dB of DG has been achieved using this configuration.
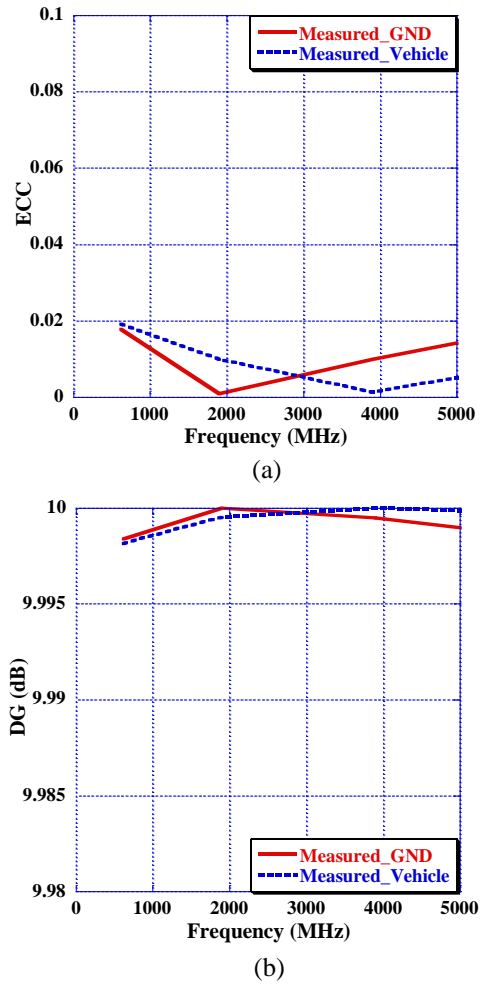

(a)

(b)

Fig. 10. Configuration II of a 2x2 MIMO system (a) ECC and (b) DG.

Figures 11 (a)-(d) presents combined radiation patterns of horizontal cuts at elevation 80 degrees for frequencies 617MHz, 1900MHz, 3900MHz and 5000MHz utilizing the same method described in subsection A.

The average gain values recorded from the combined vehicle radiation patterns are -0.71dBi, 3.16dBi, 0.57dBi, and 1.51dBi at frequencies 617MHz, 1900MHz, 3900MHz, and 5000MHz, respectively.
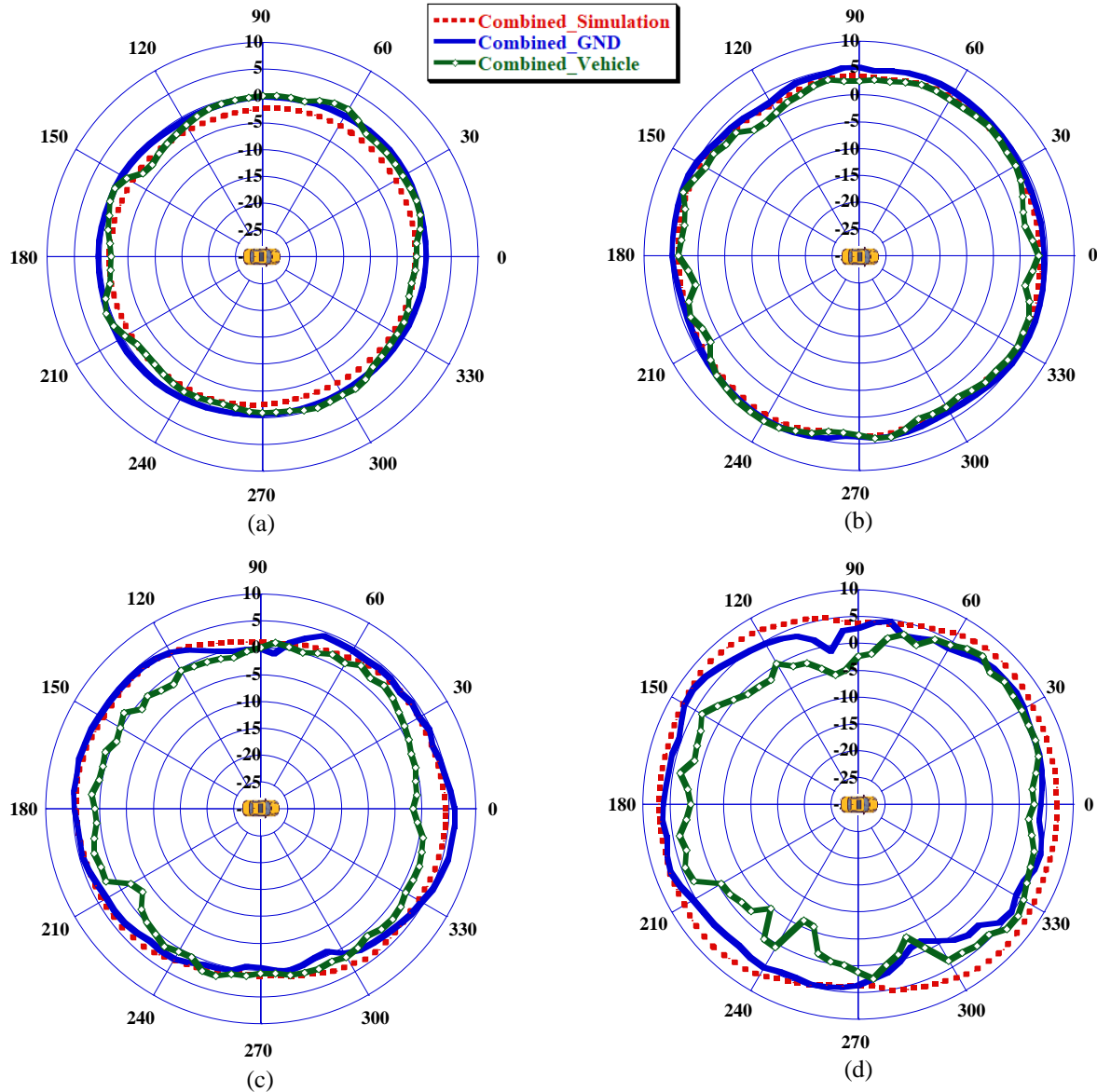
Fig. 11. Combined radiation pattern of simulation, GND measurement, and car measurement in (dBi) at theta = 80deg. for frequencies: (a) 617 MHz, (b) 1900 MHz, (c) 3900 MHz, and (d) 5000 MHz.

C. A 4x4 monopole-based MIMO system

In this subsection, four Monopole elements are integrated in the same sharkfin to operate as a 4x4 MIMO system. The building block antenna element for this configuration is the same antenna used in subsections A and B of this section. The four elements are placed in such a way that, the combined radiation pattern is omnidirectional with good isolation and correlation figures between antennas. The system placement on the car roof and simulation setup are shown in Fig. 12. The distances between Monopole pairs in this MIMO systems are listed in Table 3.
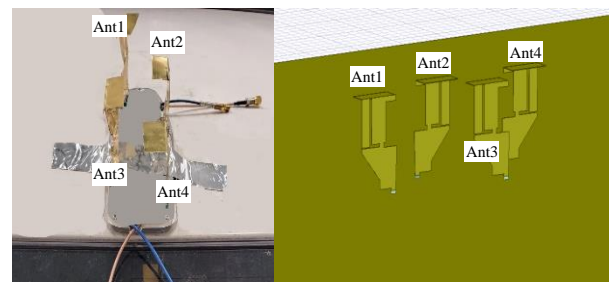

Fig. 12. A 4x4 MIMO system placement on vehicle roof and simulation setup.

Table 3. Values of the geometrical parameters of MIMO systems building block antenna

Elements Pairs	Distance (mm)
Ant1-Ant2	77
Ant1-Ant3	141
Ant1-Ant4	180
Ant2-Ant3	100
Ant2-Ant4	118
Ant3-Ant4	70

The simulated reflection coefficient (in dB) for each element in this configuration is shown in Fig. 13. The four elements from Ant1 to Ant4 shows good matching characteristics across the whole 5G bands with a reflection coefficient of less than -5.2dB and a reasonable GNSS bands rejection.

The isolation in terms of S21 between each pair of antennas within this 4x4 MIMO system is shown in Fig. 14. In general, the shorter the distance between the antennas, the worse the isolation is. However, the antenna placement and orientation also contribute to the overall isolation performance. A worse value of 10dB of isolation between Ant1-Ant2 and Ant2-Ant4 can be observed from the GND measurements on the 617-960MHz band.

Using similar approach for combining individual antennas radiation patterns as in subsection A, the combined radiation patterns at 80 degree of theta for the four elements are shown is Fig. 15. Higher average gain values are observed from the combined vehicle radiation patterns measurements compared to the other 2x2 configurations. The average gain is found to be: -0.88dBi, 4.64dBi, 3.14dBi, and 3.74dBi at frequencies 617MHz, 1900MHz, 3600MHz, and 5000MHz, respectively.
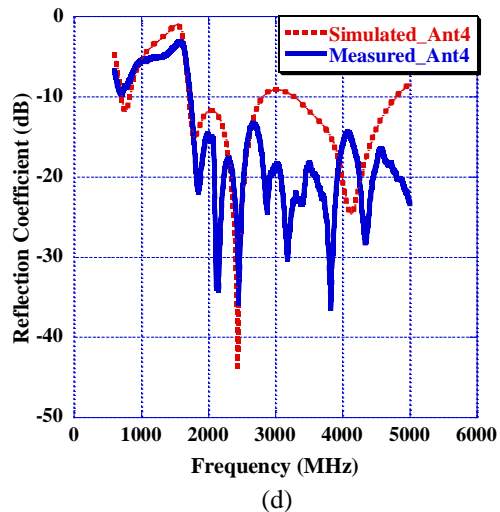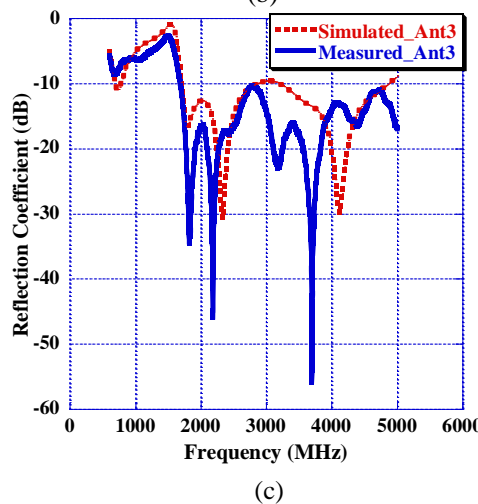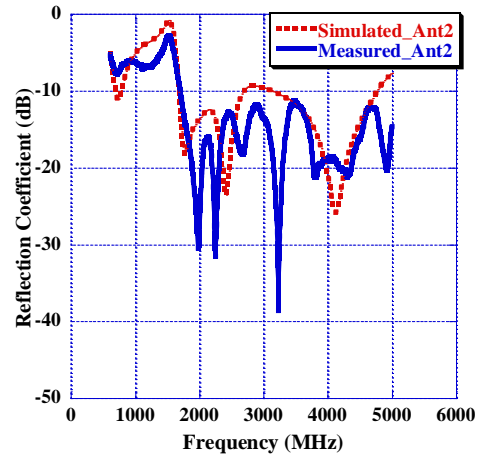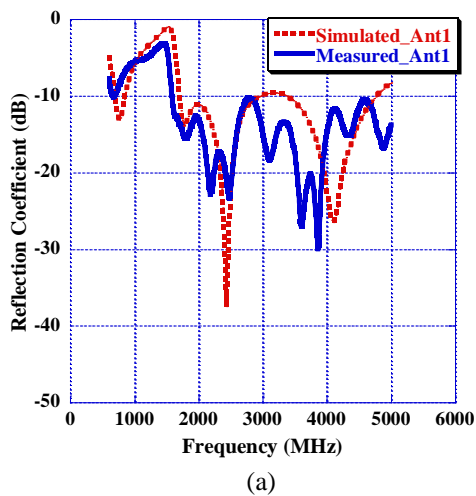

(a)

(b)

(c)

(d)

Fig. 13. 4x4 MIMO system simulated and measured reflection coefficient in dB for: (a) Antenna1, (b) Antenna2, (c) Antenna3, and (4) Antenna4.
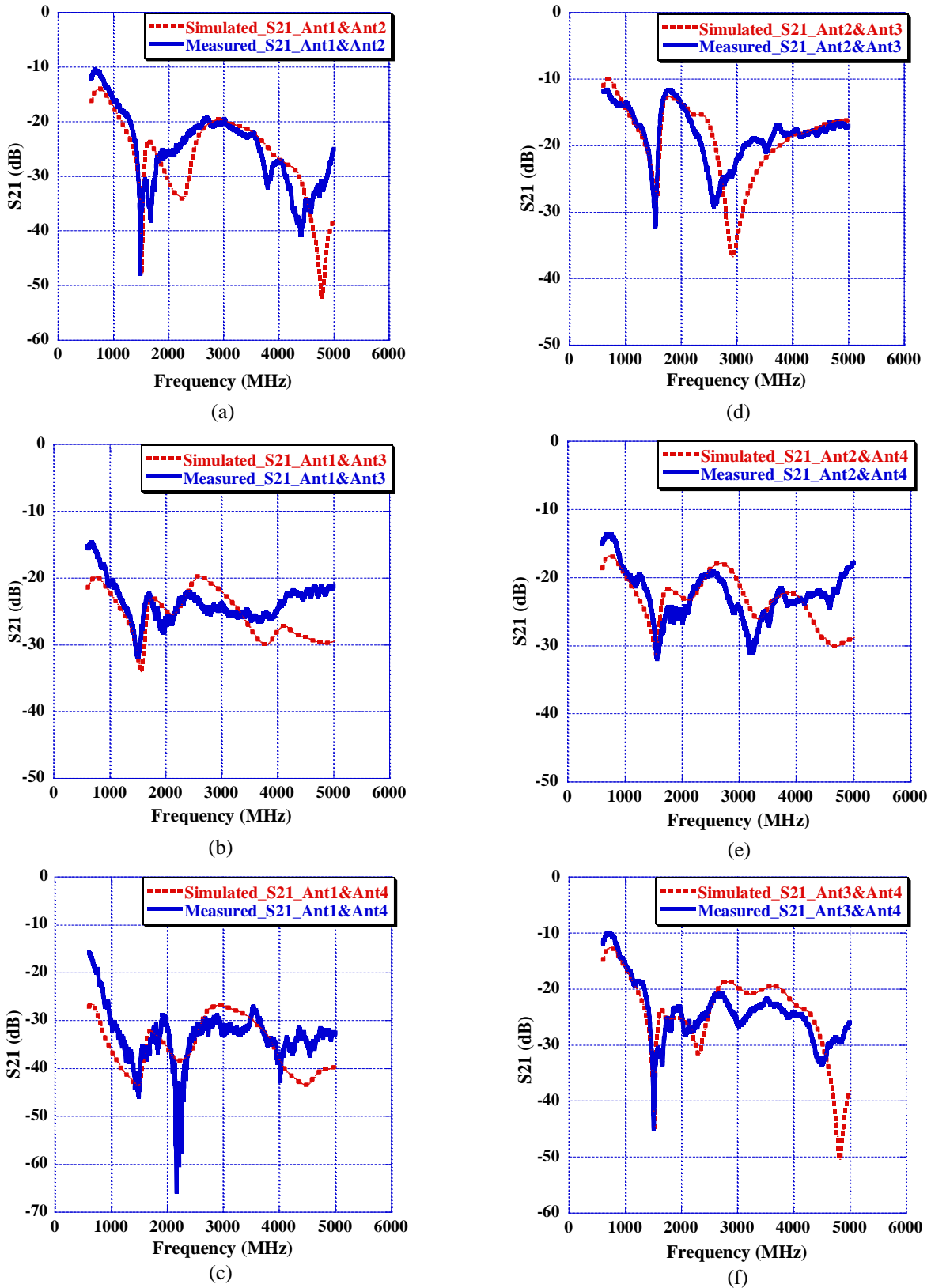
Fig. 14. 4x4 MIMO system simulated and measured Isolation in dB between: (a) Ant1 and Ant2: (b) Ant1 and Ant3; (c) Ant1 and Ant4; (d) Ant2 and Ant3; (e) Ant2 and Ant4; (f) Ant3 and Ant4.
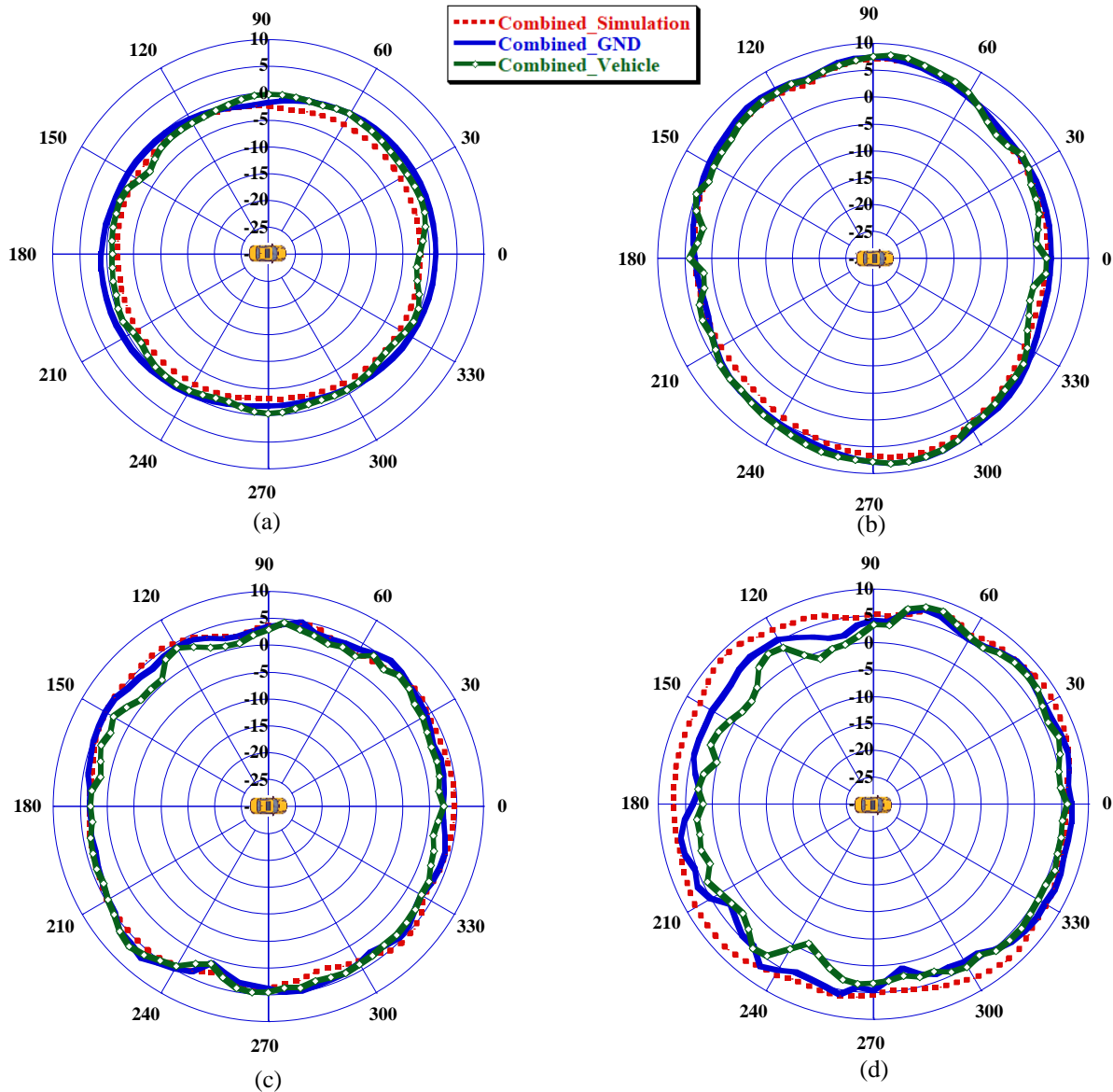
Fig. 15. Combined radiation pattern of simulation, GND measurement, and vehicle measurement in (dBi) at theta = 80 deg. for frequencies: (a) 617 MHz, (b) 1900 MHz, (c) 3900 MHz, and (d) 5000 MHz.

The on GND and on car roof measured efficiencies are reported in Figs. 16 (a), (b), and (c) for the four antenna elements in this MIMO system. It can be noticed that the GND measurement has an average total efficiency higher than 72.5% for all the four elements across the whole 5G frequency bands whereas the vehicle measurement has a reduced average total efficiency of slightly higher than 65% for all elements. The ECC and DG were also calculated in this MIMO configuration with the help of equations (1) and (2) using Octave script. As Fig. 17 suggests, the ECC is well kept

below 0.5 in all the 6 correlation cases with corresponding DG values of higher than 8.9dB. The worst value of ECC (0.45) and DG exists at low frequency bands and it is the same case where worst passive isolation occurs namely between Ant3 and Ant4.
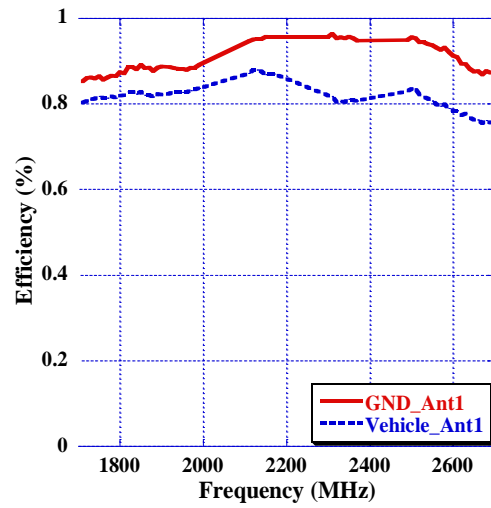
Table 4 lists a literature review summary of MIMO antennas systems used in automotive industry. The table also compares works in terms type of type of antennas, bandwidth of operations, systems volume, and method of ECC calculation in use.
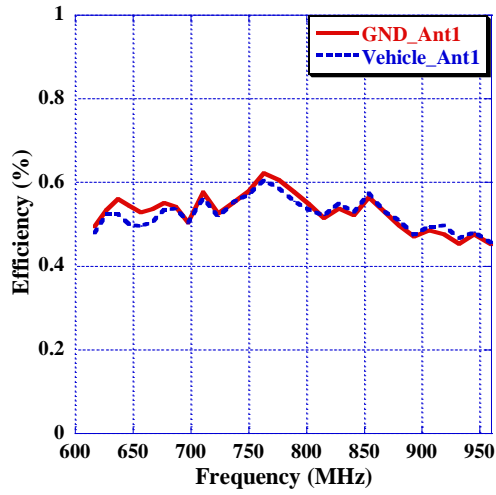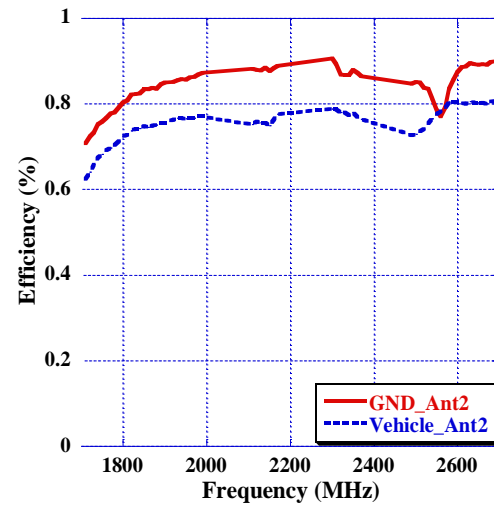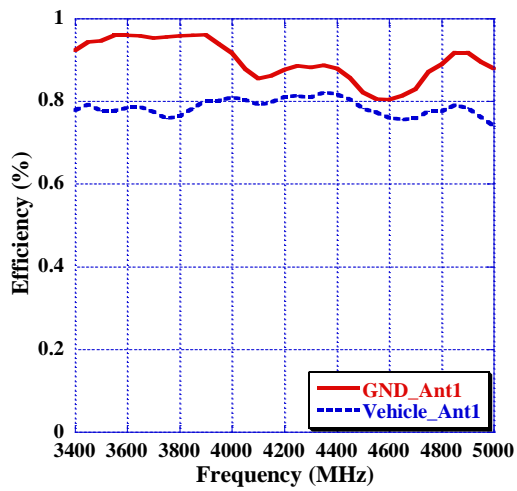
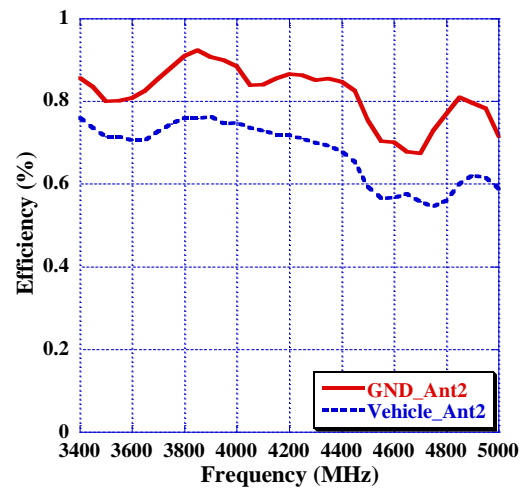(a) Ant1: 617-960MHz
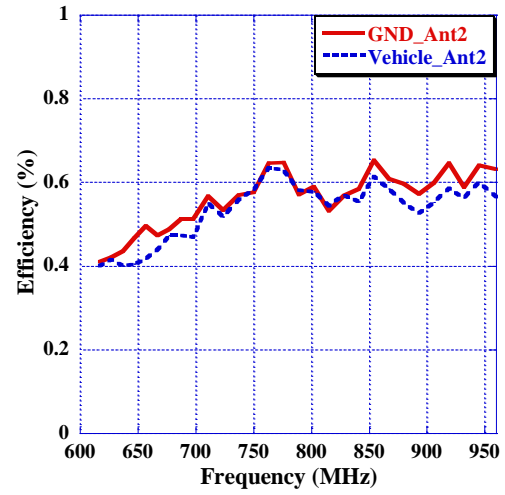
(d) Ant2: 617-960MHz
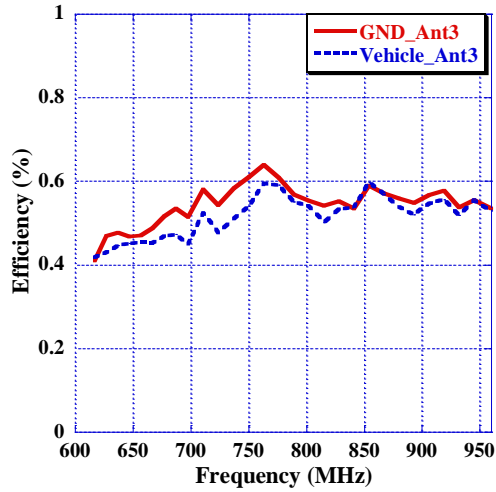
(b) Ant1: 1710-2690MHz
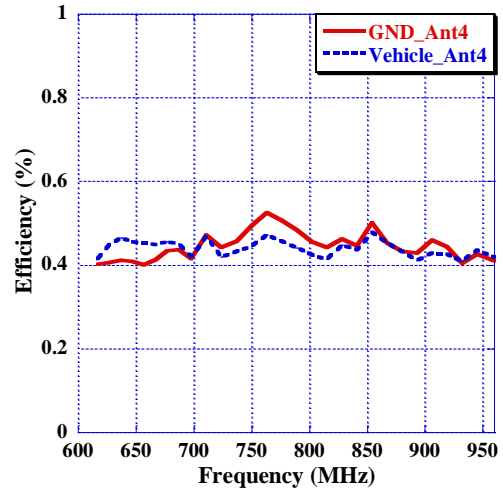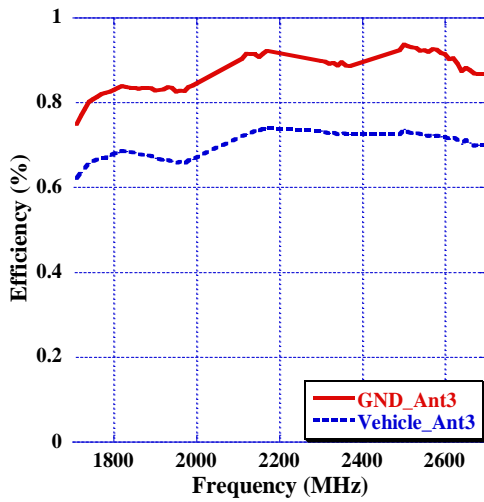
(e) Ant2: 1710-2690MHz

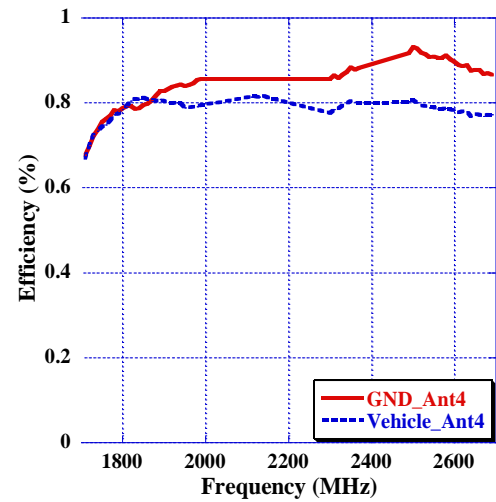(c) Ant1: 3400-5000MHz

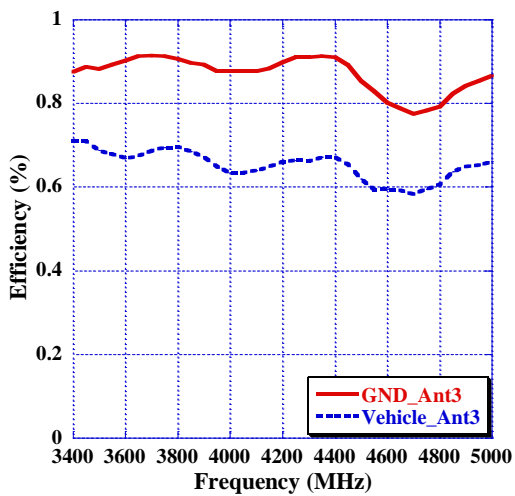(f) Ant2: 3400-5000MHz

(g) Ant3: 617-960MHz
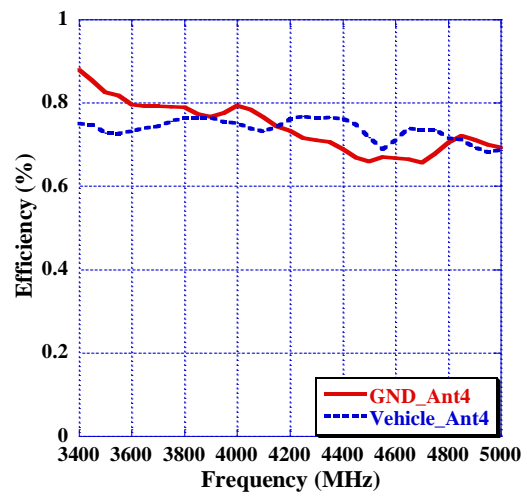
(j) Ant4: 617-960MHz

(h) Ant3: 1710-2690MHz

(k) Ant4: 1710-2690MHz

(i) Ant3: 3400-5000MHz

(l) Ant4: 3400-5000MHz
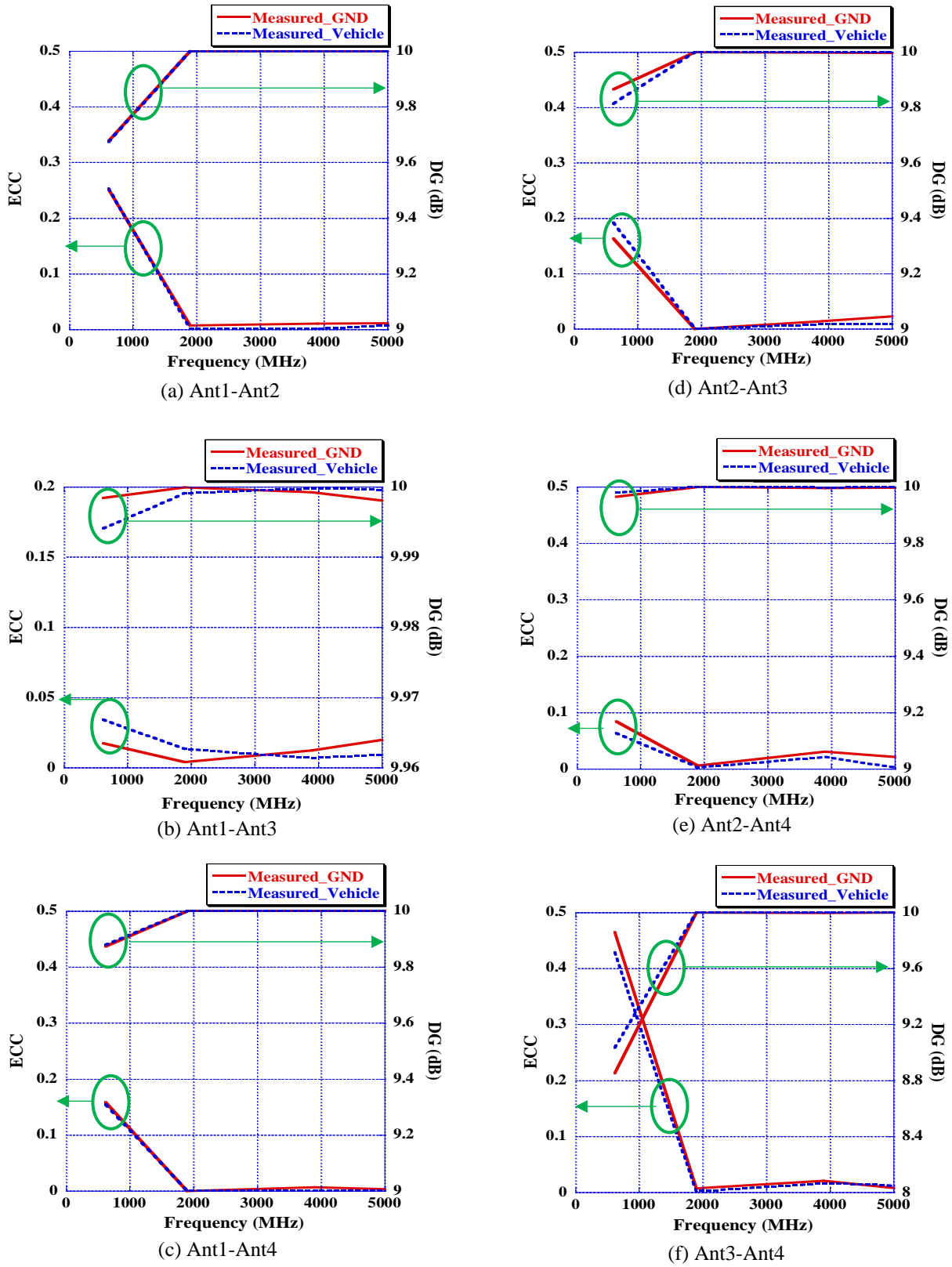
Fig. 16. Antenna efficiency for a 4x4 MIMO system.

Fig. 17. A 4x4 MIMO system ECC and DG.

Table 4: Literature review summary

Ref.	Type	BW	Antenna Dimension (LxWxH) (mm3)	ECC Method / Value
10	2x2 monopole	700MHz-900MHz	Not reported	S-param only / lower than 0.02
11	2x2 PIFA	775MHz-925MHz	59.5x12.4x21	S-param only / lower than 0.5
12	2x2 PIFA	790MHz-2.69GHz	50x50x28	E field components / lower than 0.3
13	2x2 printed monopole	790MHz-3GHz	30x0.8x80	S-param only / lower than 0.05
14	2x2 printed planar monopoles	698MHz-2700MHz	52x1.6x65	S-param only/ lower than 0.5
15	2x2 PIFA	690MHz-2700MHz	PIFA length is 75.9mm / height 25.5mm	S-param only /lower than 0.5
16	2x2 monopole	698MHz-2.69GHz	Monopole heights are 55 and 45mm	S-param only / lower than 0.5
17	2x2 printed monopoles	698MHz-2690MHz	25x2x55	Not reported / lower than 0.3
18	2x2 printed monopole PIFA	698MHz-3GHz	PIFA 65x62x20 / Monopole height is 53	Not reported
19	2x2 Nefer Antenna	700MHz-6GHz	70x70x29	S-param only / lower than 0.16
20	4x4 sleeve monopoles	790MHz-5GHz	Not reported	Not reported / lower than 0.12
29	2x2 printed Yagi	2GHz-4.5GHz	60x1.6x55	Not reported/ lower than 0.5
30	2x2 loaded monopoles	2.4GHz-11GHz	24x2.2x29	E-field components / lower than 0.02

VI. CONCLUSION

Three MIMO systems based on a novel branched Monopole structure that operates in cellular 5G bands (617MHz-5GHz) and can easily be in integrated inside a sharkfin package on a car roof have been presented in this paper. The ECC and DG derived from the radiation patterns of each antenna element were calculated for each of the three MIMO configurations. The configuration I MIMO system in Fig. 1 represents a 2x2 MIMO systems with antennas separated by a 135mm distance integrated on a sharkfin module on a car roof and it allows for a passive isolation better than 12dB, total average efficiencies higher than 71% on vehicle across all bands, ECC lower than 0.13, and DG higher than 9.9dB. The configuration II MIMO system in Fig. 7 represents a 2x2 MIMO systems with antennas separated by a 125mm distance integrated on a sharkfin module on a car roof and it provides a passive isolation better than 15dB, total average efficiencies higher than 71.7% on vehicle across all bands, ECC lower than 0.02, and DG of 10dB. Finally, in order to increase the system capacity and data rate by allowing four data streams to be sent and received simultaneously, a novel 4x4 MIMO antenna system constructed of four Monopole elements as in Fig. 12 has been designed. It achieves passive isolation better than 10dB, total average efficiencies higher than 65% on vehicle across all bands, ECC lower than 0.46, and DG higher than 8.9dB. In general, each MIMO configuration has a satisfactory performance and can be used easily in the vehicular application depending on the desired requirement and dimensions.

REFERENCES

[1] J. Malik, D. Nagpal, and M. V. Kartikeyan, "MIMO antenna with omnidirectional pattern diversity," *Electronics Letters*, vol. 52, no. 2, pp. 102-104, Jan. 2016.

[2] L. Lanctot and O. Jonah, "Cellular antenna performance impact on MIMO in vehicle," *2018 IEEE International Symposium on Antennas and Propagation & USNC/URSI National Radio Science Meeting*, Boston, MA, pp. 353-354, July 2018.

[3] A. M. Elshirkasi, A. Abdullah Al-Hadi, M. F. Mansor, R. Khan, and P. J. Soh, "Envelope correlation coefficient of a two-port MIMO terminal antenna under Uniform and Gaussian angular power spectrum with user's hand effect," *Progress in Electromagnetics Research C*, vol. 92, 123-136, Apr. 2019.

[4] S. Zhekov, A. Tatomirescu, E. Foroozanfard, and G. F. Pedersen, "Experimental investigation on the effect of user's hand proximity on a compact ultrawideband MIMO antenna array," *IET Microwaves, Antennas Propag.*, vol. 10, no. 13, pp. 1402-1410, Oct. 2016.

[5] L. L. Nagy, *Automobile Antennas*, McGraw-Hill, New York, 2007.

[6] K. L. Wong, *Planar Antennas for Wireless Communications*, Wiley Interscience, Hoboken, NJ, Jan. 2003.

[7] V. Rabinovich, N. Alexandrov, and B. Alkhateeb, *Automotive Antenna Design and Applications*, CRC Press, Taylor & Francis, Boca Raton, FL, Dec. 2017.

[8] S. Arianos, G. Dassano, F. Vipiana and M. Orefice, "Design of multi-frequency compact antennas for automotive communications," *IEEE Transactions on Antennas and Propagation*, vol. 60, no. 12, pp. 5604-5612, Dec. 2012.

[9] G. Artner, W. Kotterman, G. Del Galdo, and M. A. Hein, "Automotive antenna roof for cooperative connected driving," *IEEE Access*, vol. 7, pp. 20083-20090, Jan. 2019.

[10] H. J. Song, A. Bekaryan, J. H. Schaffner, T. Talty, D. Carper, E. Yasan, and A. Duzdar, "Evaluation of vehicle-level MIMO antennas: capacity, total embedded efficiency, and envelope correlation," *2014 IEEE-APS Topical Conference on Antennas and Propagation in Wireless Communications (APWC)*, Palm Beach, FL, pp. 89-92, Aug. 2014.

[11] O. Kwon, R. Song, and B. Kim, "A fully integrated shark-fin antenna for MIMO-LTE, GPS, WLAN, and WAVE applications," *IEEE Antennas and Wireless Propagation Letters*, vol. 17, no. 4, pp. 600-603, Apr. 2018.

[12] V. Franchina, A. Michel, P. Nepa, M. Gallo, R. Parolari, A. P. Filisan, and D. Zamberlan, "A compact 3D antenna for automotive LTE MIMO applications," *2017 IEEE-APS Topical Conference on Antennas and Propagation in Wireless Communications (APWC)*, Verona, Italy, pp. 326-329, Oct. 2017.

[13] A. Heiman, A. Badescu, and A. Saftoiu, "A new multiple input multiple output V2V automotive antenna for long term evolution band applications," *2018 International Symposium on Fundamentals of Electrical Engineering (ISFEE)*, Bucharest, Romania, pp. 1-5, Nov. 2018.

[14] D. Preradovic and D. N. Aloi, "Cross polarized 2x2 LTE MIMO system for automotive shark fin application," *The Applied Computational Electromagnetics Society (ACES)*, vol. 35, no. 10, pp. 1207-1216, Oct. 2020.

[15] C. Demien and R. Sarkis, "Design of shark fin integrated antenna systems for automotive applications," *2019 PhotonIcs & Electromagnetics Research Symposium - Spring (PIERS-Spring)*, Rome, Italy, pp. 620-627, June 2019.

[16] A. Thiel, L. Ekiz, O. Klemp, and M. Schultz, "Automotive grade MIMO antenna setup and performance evaluation for LTE-communications," *2013 International Workshop on Antenna Technology (iWAT)*, Karlsruhe, pp. 171-174, Mar. 2013.

[17] Y. Liu, Z. Ai, G. Liu, and Y. Jia, "An Integrated shark-fin antenna for MIMO-LTE, FM, and GPS applications," *IEEE Antennas and Wireless Propagation Letters*, vol. 18, no. 8, pp. 1666-1670, Aug. 2019.

[18] N. Guan, H. Tayama, M. Ueyama, Y. Yoshijima, and H. Chiba, "A roof automobile module for LTE-MIMO antennas," *2015 IEEE-APS Topical Conference on Antennas and Propagation in Wireless Communications (APWC)*, Turin, pp. 387-391, Sep. 2015.

[19] S. Hastürkoğlu, M. Almarashli, and S. Lindenmeier, "A compact wideband terrestial MIMO-Antenna set for 4G, 5G, WLAN and V2X and evaluation of its LTE-Performance in an urban region," *2019 13th European Conference on Antennas and Propagation (EuCAP)*, Krakow, Poland, pp. 1-5, Mar. 2019.

[20] O. Jonah, "5G antenna for automotive applications," *2020 IEEE International Symposium on Antennas and Propagation and North American Radio Science Meeting*, pp. 1493-1494, Web, July 2020.

[21] T. Jiang, T. Jiao, and Y. Li, "A low mutual coupling MIMO antenna using periodic multi-layered electromagnetic band gap structures," *The Applied Computational Electromagnetics Society (ACES)*, vol. 33, no. 3, Mar. 2018.

[22] F. Liu, J. Guo, L. Zhao, G. Huang, Y. Li, and Y. Yin "Ceramic superstrate-based decoupling method for two closely packed antennas with cross-polarization suppression," *IEEE Transactions on Antennas and Propagation*, vol. 69, no. 3, pp. 1751-1756, Mar. 2021.

[23] S. Luo, Y. Li, Y. Xia, G. Yang, L. Sun, and L. Zhao, "Mutual coupling reduction of a dual-band antenna array using dual-frequency metamaterial structure," *The Applied Computational Electromagnetics Society (ACES)*, vol. 34, no. 3, pp. 403-410, Mar. 2019.

[24] A. Mansoor and R. Amiri, "Mutual coupling reduction of closely spaced MIMO antenna using frequency selective surface based on meta-materials," *The Applied Computational Electromagnetics Society (ACES)*, vol. 32, no. 12, pp. 1064-1068, Dec. 2017.

[25] K. Yu, Y. Li, and X. Liu, "Mutual coupling reduction of a MIMO antenna array using 3-D novel meta-material structures," *The Applied Computational Electromagnetics Society (ACES)*, vol. 33, no. 7, pp. 758-763, July 2018.

[26] S. Luo, Y. Li, Y. Xia, and L. Zhang "A low mutual coupling antenna array with gain enhancement using metamaterial loading and neutralization line structure," *The Applied Computational Electromagnetics Society (ACES)*, vol. 34, no. 3, pp. 411-418, Mar. 2019.

[27] J. Jiang, Y. Xia, and Y. Li "High isolated X-band MIMO array using novel wheel-like metamaterial decoupling structure," *The Applied Computational Electromagnetics Society (ACES)*, vol. 34, no. 12, pp. 1829-1836, Dec. 2019.

[28] S. F. Beegum and S. K. Mishra, "Compact WLAN band-notched printed ultrawideband MIMO antenna with polarization diversity," *Progress in Electromagnetics Research C*, vol. 61, pp. 149-159, Jan. 2016.

[29] K. Sreelakshmi, P. Bora, M. Mudaliar, Y. Dhanade, and B. T. P. Madhav, "Linear array Yagi-Uda 5G antenna for vehicular application," *International Journal of Engineering & Technology*, vol. 7. pp. 513-517, Dec. 2017.

[30] D. Potti, Y. Tusharika, M. G. N. Alsath, S. Kirubaveni, M. Kanagasabai, R. Sankararajan, S. Narendhiran, and P. B. Bhargav, "A novel optically transparent UWB antenna for automotive MIMO communications," *IEEE Transactions on Antennas and Propagation*, vol. 69, pp. 3821-3828, July 2021.

Mohamed O. Khalifa received the B.S. degree in Electrical and Electronic Engineering from University of Khartoum, Khartoum, Sudan, in 2010 and the M.S. degree in Electrical Engineering from King Fahd University of Petroleum and Minerals, Dhahran, KSA, in 2015. He is currently pursuing the Ph.D. degree in Electrical and Computer Engineering at Oakland University.

He served as a Research Assistant at King Fahd University of Petroleum and Minerals, Visiting graduate Intern at I-Radio Lab within the School of Engineering at University of Calgary in Alberta, Canada and Research Assistant at Applied EMAG and Wireless Lab at Oakland University from 2012-2018. He has been employed in Ficosa North America, Madison Heights, Michigan from 2018-2019 then in Molex LLC, Grand Blanc, Michigan from 2019 until present. His research interests reside in area of Power Amplifier design and linearization techniques and applied electromagnetics with emphasis on antenna measurements, antenna modeling/analysis and antenna design. He has authored/co-authored around 10 technical papers and is an inventor on 3 patents.

Ahmad M. Yacoub received the B.S. degree in Electrical Engineering from Princess Sumaya University for Technology Amman, Jordan, in 2014 and the M.S. degree in Electrical and Computer Engineering from Oakland University, Rochester, Michigan, in 2018. He is currently pursuing the Ph.D. degree in Electrical and Computer Engineering at Oakland University.

He served as a Research Assistant at Applied EMAG and Wireless lab at Oakland University from 2016-2018. He has been employed in Molex LLC, Grand Blanc, Michigan from 2018 until present. Yacoub's research interests reside in area of applied electromagnetics with emphasis on antenna measurements, antenna modeling/analysis and antenna design. He is an inventor/co-inventor of 2 patents.

Daniel N. Aloi received his B.S. (1992), M.S. (1996) and Ph.D. (1999) degrees in Electrical Engineering from Ohio University, located in Athens, Ohio, USA. He served as a Research Assistant from 1995-1999 in the Avionics Engineering Center within the School of Engineering and Computer Science at Ohio University; Summer Intern at Rockwell International in Cedar Rapids, Iowa, and Senior Project Engineer at OnStar, Incorporated, a subsidiary of General Motors from 2000-2002. He has been employed in the Electrical and Computer Engineering Department at Oakland University in Rochester, Michigan from 2002 until present. He is the Founder and Director of the Applied EMAG and Wireless Lab at Oakland University.

Aloi's research interests reside in area of applied electromagnetics with emphasis on antenna measurements, antenna modeling/analysis and antenna design. He is a member of the Institute of Navigation and is a senior member of the Institute of Electrical and Electronics Engineers (IEEE). He has received in excess of $4M in research funding from a variety of federal and private entities including the Federal Aviation Administration, Defense Advanced Research Program Agency (DARPA) and the National Science Foundation (NSF). He has authored/co-authored over 100 technical papers and is an inventor on 5 patents.